



# Optical, conductivity and dielectric properties of plasticized solid polymer electrolytes based on blends of sodium carboxymethyl cellulose and polyethylene oxide

Rania Badry<sup>1</sup> · Sherif El-Khodary<sup>2</sup> · Hanan Elhaes<sup>1</sup> · Nadra Nada<sup>1</sup> · Medhat Ibrahim<sup>3</sup>

Received: 4 April 2020 / Accepted: 20 November 2020 / Published online: 28 November 2020  
© Springer Science+Business Media, LLC, part of Springer Nature 2020

## Abstract

Solid polymer electrolytes (SPEs) based on plasticized sodium carboxymethyl cellulose/polyethylene oxide (CMC/PEO) were successfully prepared using solution casting method. The prepared SPEs were investigated using different spectroscopic techniques. Ultraviolet–Visible absorption spectra (UV–Vis) revealed that changing PEO content in the polymer matrix causes the optical band gap energy to change and decrease. These changes indicate that there is a transfer of charge carriers within the polymer matrix. The variations occurring in the major structural units within the prepared CMC/PEO SPEs are retraced using Fourier transform infrared spectroscopy (FTIR). FTIR results revealed that the polymeric materials suffer changes in their chemical structures and that complexation occurred between the individual polymers due to blending. Correlation between UV–Vis optical band gap and FTIR outcomes is established. Electrical impedance spectroscopy (EIS) was used to study the conduction mechanism for the prepared SPEs. Impedance results showed that the CMC/PEO sample with blending ratio of 80/20 wt% (sample named B2) possesses the highest ionic conductivity of  $1.18\text{E}-06$  S/cm and the lowest activation energy of approximately 0.67 eV at ambient temperature.

**Keywords** CMC · PEO · UV–Vis · Absorption · FTIR · EIS

## 1 Introduction

Blending of polymers is considered as the most important process for creating new electric materials as it can increase the amorphous fractions in the polymeric materials. Also, blending can be used to develop materials with a massive new property to be used as

---

✉ Medhat Ibrahim  
medahmed6@yahoo.com

<sup>1</sup> Physics Department, Faculty of Women for Arts, Science and Education, Ain Shams University, 11757 Cairo, Egypt

<sup>2</sup> Building Physics and Environment Institute, Housing and Building National Research Center (HBRC), 12311 Dokki, Giza, Egypt

<sup>3</sup> Molecular Spectroscopy and Modeling Unit, Spectroscopy Department, National Research Centre, 33 El-Bohouth St., 12622 Dokki, Giza, Egypt

polymer electrolytes (Selvasekarapandian et al. 2006; Kumar et al. 2014). Blending of polymeric materials became a costless, simple, easy, and non-toxic method for polymer preparation to compensate the industrial needs (Mishra et al. 2018a, b; Choudhary 2018). In the fields of material science, physics and chemistry, blending process is considered as a promising method for preparation of polymers especially in capacitors, solar cells, batteries and fuel cells based on the study of their optical and electrical properties (Ngai et al. 2016; Li et al. 2017; Mohan et al. 2007; Meyer 1998). Based on the literature, by changing the way of polymer blending, miscibility degree and the ratio of the compositions, the properties of the outcomes of blending polymers can be varied (Rajah et al. 2019; Kayyarapu and Chekuri 2018).

The first synthetic polymer used as a polymer electrolyte is polyethylene oxide (PEO). PEO is a semi-crystalline linear chain polymer and has a lot of features as being a non-toxic, thermally stable, flexible, hydrophilic, and cost-effective polymer (Choudhary 2016; Morsi et al. 2018). Despite all these advantages of PEO, it possesses a poor ionic conductivity due to its high crystallinity and therefore it is impossible for it to achieve a high DC conductivity. The poor ionic conductivity of PEO can be enhanced with the addition of plasticizer, acid, salt, another conductive polymer or increasing temperature (Li et al. 2017; Dabbak et al. 2018; Armand 1986; Nasution et al. 2017). However, it is well known that PEO is the best polymeric material suitable for electrolytes based on solid polymers (Srivastava and Tiwari 2009). Abdulrazak (2018), prepared a polymer blend from PEO/PVP and the results indicated that the optical band gap is influenced strongly by the incorporation of silver nanoparticles.

Therefore, sodium carboxymethyl cellulose (CMC) is chosen here to form a blend with PEO to increase the amorphous fractions within PEO as CMC is a semi-crystalline polymer (Brako et al. 2015). As these two polymers have a common solvent (water), a strong interaction between CMC and PEO takes place via the ether (–O–) group of PEO and both carboxylic and hydroxyl groups of CMC (Choudhary 2018; dabbed, Dabbak et al. 2018; El-Sayed et al. 2011; Gupta et al. 2013). CMC is a natural, polysaccharide, organic and nontoxic polymer (Kargarzadeh et al. 2012). Also, CMC participates in many industrial applications like food, paper, paints, cosmetics, and pharmaceuticals (El-Bana et al. 2018; Morsi et al. 2018, 2019).

The aim of the present study is to introduce a new solid polymer electrolyte based on plasticized CMC/PEO blends. By controlling the crystalline regions of PEO and the amorphous ones of CMC, new compositions of CMC/PEO suitable for optoelectronic and photonic devices can be obtained. The major aim of the present work is also to study the optical properties and the electrets resulting from the blending process. For accurate determination of the transition type of electrons, studying the optical dielectric loss is employed.

## 2 Experimental

### 2.1 Materials

CMC with average molecular weight of  $2.5 \times 10^5$  g/mol is purchased from K. Patel Chemopharma PVT, India. PEO with average molecular weight of  $4 \times 10^4$  g/mol was acquired from ACROS, New Jersey, USA. All the studied solid polymer electrolytes are prepared using distilled water as a common solvent.

## 2.2 Preparation of CMC/PEO SPEs

SPEs based on CMC/PEO were prepared using solution casting technique. 2 gm of CMC were dissolved in 150 ml distilled water in one beaker and stirred using a magnetic stirrer for 8 h until complete mixing. While 2 gm from PEO were dissolved in 100 ml distilled water separately and stirred for 2 h. After complete mixing of both solutions separately, SPE films were prepared by mixing different concentrations of CMC/PEO following the sequence of 90/10, 80/20, 70/30 and 60/40 respectively, and stirred for additional 6 h. Constant amount of glycerol (40 wt% based on literature) was added to each sample to enhance the mechanical properties of CMC/PEO films. All SPEs were prepared at room temperature as presented in Table 1. Finally, the clear viscous solutions of blended CMC/PEO were put in glass petri dishes and left to dry in air for approximately 5 days.

## 2.3 Measurements

The prepared SPEs of CMC/PEO blends were characterized using UV–Vis. absorption spectroscopy using a double beam spectrophotometer, JASCO model V-670 in the spectral regions of UV–Vis-NIR, at Spectroscopy Department, National Research Centre (NRC), Cairo, Egypt. Attenuated total reflection (ATR) FTIR spectra of CMC, PEO and CMC/PEO were obtained using Vertex 70 FTIR spectrometer from Bruker Optic GmbH, Germany, equipped with diamond ATR crystal system in the spectral range of 4000–400  $\text{cm}^{-1}$  with the resolution of 4  $\text{cm}^{-1}$ , at Spectroscopy Department, NRC, Cairo, Egypt. The AC conductivity of CMC/PEO blends were measured in the frequency range of 50 Hz–5 MHz at several temperatures from 298 K to 388 K using HIOKI 3532-50 LCR Hi-Tester bridge at Building Physics and Environment Institute, Housing & Building National Research Center (HBRC), Dokki, Giza, Egypt.

## 3 Results and discussion

### 3.1 UV–Vis results

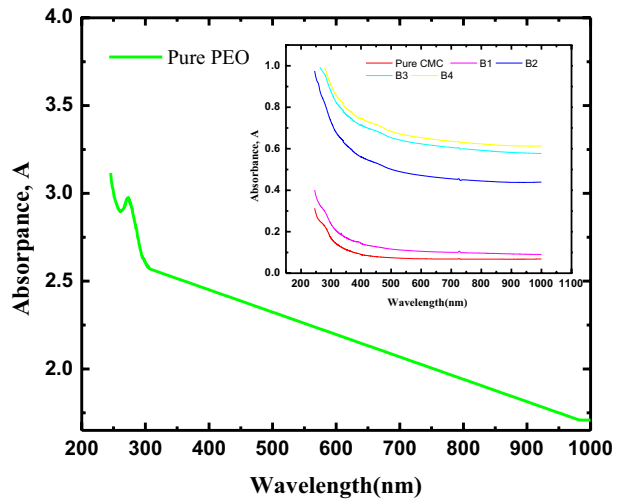
#### 3.1.1 UV–Vis absorption spectra analysis

Studying the absorption spectra of organic polymers optically gives information about the band structure of such materials. Figure 1 presents the absorption UV–Vis spectra of pure

**Table 1** Abbreviation of each blended sample with the content of both CMC and PEO

Sample	Water (ml)	Plasticizer (Glycerol)	CMC (wt %)	PEO (wt %)
CMC	150	(40 wt%)	100	0
B1	–	(40 wt%)	90	10
B2	–	(40 wt%)	80	20
B3	–	(40 wt%)	70	30
B4	–	(40 wt%)	60	40
PEO	100	(40 wt%)	0	100

**Fig. 1 a and b** UV–Vis. absorption spectra of pure CMC, pure PEO and CMC blended with PEO at different ratios as (90:10, 80:20, 70:30 and 60:40)



CMC, pure PEO and CMC blended with PEO in the wavelength range 200 to 1000 nm. Optical characterization of all samples is collected by the main observed absorption edge/shoulder that undergoes shift towards the lower energy range due to blending. The edge red shift, presented in the figure, refers to the complexation occurred between the individual polymers due to blending. Also, the shift may be attributed to the changes that occurred in the degree of amorphousity/crystallinity upon blending (Sengwa and Choudhary 2017; Sharma et al. 2013; Kumar 2014).

As depicted in the figure, PEO has an absorption peak at approximately 272 nm which may be due to  $\pi \rightarrow \pi^*$  transition. This absorption peak is disappeared with the substitution of different amounts of CMC. Moreover, it is clear from the figure that the absorbance of CMC film is changed slightly with the addition of PEO. However, it is noticed also that the absorbance of blended CMC/PEO decreased with decreasing the energy of the incident photons.

### 3.1.2 Optical energy band gap determination ( $E_g$ )

As CMC and PEO are semi-crystalline polymers, which means that they can be classified as direct band gap semi-conductors or indirect band gap semi-conductors. Direct band gap semi-conductors have the valence band top correspond to the conduction band bottom which means that direct band gap materials have the same wave vector. However, indirect band gap semi-conductors do not possess the same wave vector as the bands do not correspond to each other (Davis and Mott 1970; Dabbak et al. 2018).

Davis and Mott reported that both direct and indirect transitions of electrons take place near the edge of the fundamental band of absorption. The two types of transitions can be observed by drawing  $(\alpha h\nu)^2$  and  $(\alpha h\nu)^{1/2}$  as a function of photon energy by extrapolating the straight line of each curve to the X-axis. This extrapolation method for the calculation of the energy gap is widely and effectively used for both polymeric and inorganic materials (Figa et al. 2009, 2019; Kuly et al. 2013). However, for the studied polymers, it is stated that the electrons follow indirect allowed transition between the valence and conduction bands (Chahal et al. 2012; Ling et al. 2016; Mott 1970).

Accordingly, the variation of  $(\alpha h\nu)^{1/2}$  with the incident energy is presented in Fig. 2. The figure shows that the blended samples possess two band gaps. Badry et al. 2020 determined the optical band gap energy of pure CMC and it is concluded that CMC possesses three band gaps which are 1.52, 3.24 and 4.7 eV.

Using the model proposed by both Davis and Mott, the transition type and the energy gap values are determined using the following equations (Davis and Mott 1970):

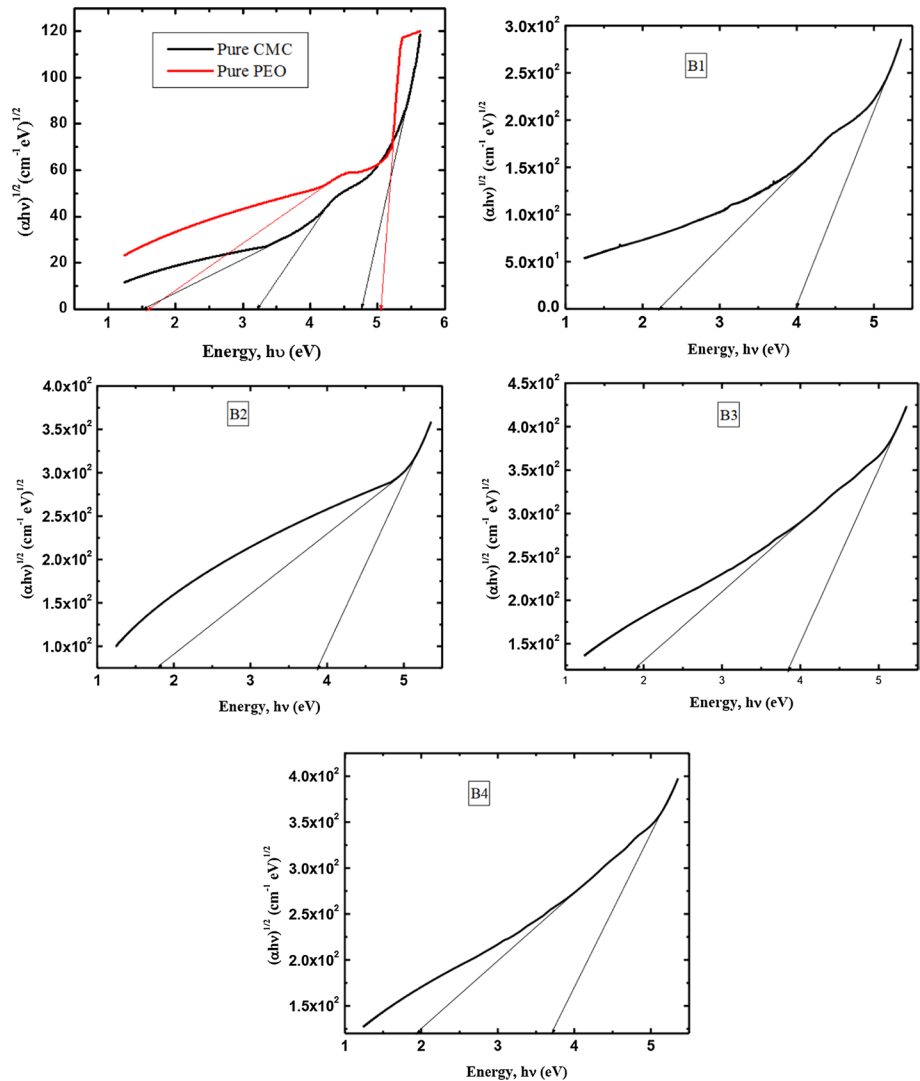


**Fig. 2** Indirect allowed transitions  $(\alpha h\nu)^{1/2}$  versus photon energy ( $h\nu$ ) for pure CMC, pure PEO and CMC blended with PEO at different ratios as (90:10, 80:20, 70:30 and 60:40)

$$(\alpha h\nu)^2 = B(h\nu - E_{gd}) \quad \text{For direct allowed transitions}$$

$$(\alpha h\nu)^{1/2} = B(h\nu - E_{gi}) \quad \text{For indirect allowed transitions}$$

where  $h\nu$  is the photon energy,  $E_g$  is the optical energy gap and  $\alpha$  is the absorption coefficient (Fartode et al. 2015). Beer-Lambert law stated that the coefficient of absorption ( $\alpha$ ) can be determined using the following relation:

$$\alpha = 2.303 (A/L) \quad (1)$$

where  $\alpha$  is the absorption coefficient,  $A$  is the sample absorbance and  $L$  is the thickness of the SPE films (Sengwa and Choudhary 2017; Dabbak et al. 2018;). The optical energy gaps for the prepared SPEs based on CMC/PEO are presented in Table 2. As presented in the table, the PEO band gap underwent a sharp increase giving the values of 2.23, 1.8, 1.9 and 1.95 eV for B1, B2, B3 and B4, respectively. Meanwhile, the second edge for optical absorption gave another gap at 4, 3.82, 3.99 and 3.84 eV for samples B1, B2, B3 and B4, respectively. This decrease in the band gap values of pure CMC and those of pure PEO upon blending indicates that the amorphous regions are increased, and that the optical conductivity was also enhanced.

A resultant influence has been observed on the optical band gap of CMC/PEO SPEs by PEO increment into the plasticized CMC. PEO caused the formation of some defects in the plasticized films, as shown in Fig. 2, for indirect allowed transitions, where localized levels are created within the SPE optical band gap due to the formation of defects. The density of such levels is proportional to the concentration of the defects within the prepared SPEs (Mott 1970; Murri et al. 1992; Samsudin and Isa 2012; Masoud et al. 2013). The blending process may cause overlapping of these localized levels. This overlap confirms the decrease in the optical energy band gap by increasing PEO concentration in the polymer matrix as presented by Badry et al. 2020 and Zhu et al. 2014. Additionally, it is reported that this reduction in the optical band gap values can be proven by the increase occurring in the degree of amorphousity (Murri et al. 1992; Samsudin and Isa 2012). The changes occurring in the values of the optical energy band gaps may be attributed to the chemical bonds formed between the CMC chain and PEO chain. This change in the optical energy gaps means that CMC/PEO SPEs became more sensitive and can be used in sensing devices as a membrane material.

### 3.2 FTIR results

Complexation between the individual polymers upon blending can be confirmed by FTIR spectroscopy. Figure 3 presents the FTIR spectra of pristine PEO. The FTIR absorption spectra of all the blended samples are presented in Fig. 4 in the same spectral region. The

**Table 2** Indirect band gap energies of pure PEO and CMC blended with PEO as (90:10, 80:20, 70:30 and 60:40)

Sample	$E_1$ (eV)	$E_2$ (eV)
PEO	1.54	5.07
B1	2.23	4
B2	1.8	3.82
B3	1.9	3.99
B4	1.95	3.84

**Fig. 3** The FTIR spectrum of pure PEO

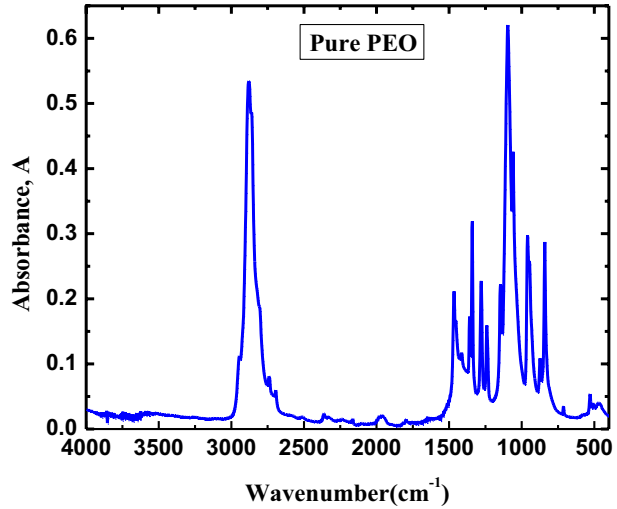
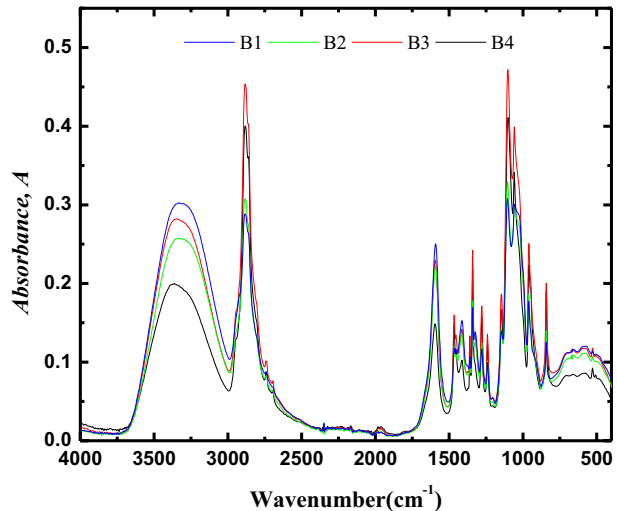


**Fig. 4** FTIR spectra for all blended CMC/PEO samples as (90:10, 80:20, 70:30 and 60:40)



assignment for all absorption bands of pure PEO and those of all blended samples, based on the position of the characteristic bands, are presented in Tables 3 and 4 respectively (Sengwa et al. 2010; Ling et al. 2016).

FTIR spectra of CMC are compatible with those announced previously (Badry et al. 2020). For the FTIR spectra of pristine polymers, the presence of C=O and O-H group in CMC and the ether group (C-O-C) in the highly negative PEO enables them to have a strong tendency to form hydrogen bonds with each other upon blending and are considered as good acceptors for protons due to the presence of such functional groups in their structures (Fartode et al. 2015; Gupta et al. 2013; Kumar et al. 2016).

The absorption spectra of all prepared SPEs based on CMC/PEO blends show the major functional groups of both CMC and PEO such as O-H stretching, C-H asymmetrical stretching of CH<sub>3</sub> and COO<sup>-</sup> stretching for CMC, and it is observed that

**Table 3** FTIR assignment of pure PEO

Wavenumber (cm <sup>-1</sup> )	Assignment
2879	C–H symmetrical stretching of CH <sub>3</sub>
2694	Asymmetric C–H stretching of CH <sub>2</sub>
1961	C–H asymmetrical stretching of CH <sub>3</sub>
1466	C–H bending of CH <sub>2</sub>
1359	C–H bending of CH <sub>3</sub>
1279	C–O asymmetric stretching
1241	C–O symmetric stretching
1146	–C–O–C- asymmetric stretching
1096	–C–O–C- symmetric stretching
1059	CH–O–CH <sub>2</sub> stretching
960	CH <sub>2</sub> asymmetric rocking
841	CH <sub>2</sub> symmetric rocking

**Table 4** FTIR assignment of CMC blended with PEO as (90:10, 80:20, 70:30 and 60:40)

B1	B2	B3	B4	Assignment
Wavenumber (cm <sup>-1</sup> )				
3329	3342	3347	3363	OH stretching
2883	2884	2883	2883	CH symmetric stretching of CH <sub>3</sub>
1592	1593	1594	1596	COO stretching of carboxylic group of CMCs
1465	1465	1465	1465	CH <sub>2</sub> bending of PEO
1414	1414	1414	1414	CH <sub>2</sub> bending of CMC
1360	1360	1359	1359	CH <sub>3</sub> bending of PEO
1341	1341	1341	1341	CH <sub>2</sub> asymmetric wagging [new]
1321	1321	1321	1321	OH, bending of CMC
1279	1279	1279	1279	C–O asymmetric stretching of PEO
1241	1241	1241	1241	C–O symmetric stretching of PEO
1146	1147	1147	1146	–C–O–C- asymmetric stretching
1105	1104	1103	1100	–C–O–C- symmetric Stretching
1057	1058	1050	1059	CH–O–CH <sub>2</sub> stretching
961	961	960	960	CH <sub>2</sub> asymmetric rocking
842	842	842	842	CH <sub>2</sub> symmetric rocking

by decreasing the CMC content in the blended films, the intensity of such bands (3285 cm<sup>-1</sup>, 1589 cm<sup>-1</sup>, 1414 cm<sup>-1</sup> and 1321 cm<sup>-1</sup>) decreased. While for PEO, C-H symmetrical and C-H asymmetrical stretching are observed at 2879 cm<sup>-1</sup> and 2694 cm<sup>-1</sup> respectively. However, the bands at 1961 cm<sup>-1</sup>, 1466 cm<sup>-1</sup> and 1359 cm<sup>-1</sup> are attributed to C-H bending vibrations, the bands at 1279 cm<sup>-1</sup> and 1241 cm<sup>-1</sup> are corresponding to C-O stretching vibrations (the region of 1200-1300 cm<sup>-1</sup> is mostly due to C-O stretching), and finally -C-O-C- asymmetric and symmetric stretching are observed at 960 cm<sup>-1</sup>, and 841 cm<sup>-1</sup> respectively. Also, the absorption of these bands was found to increase with increasing PEO concentration in the prepared films.



Furthermore, the effect of blending can be observed from the decrease or increase in the intensity of absorption bands, band broadening and band shift to higher wavenumbers which refer to that a complex interaction between COO and OH of CMC and the oxygen atoms of PEO has occurred. Also, there is a new band observed at  $1341\text{ cm}^{-1}$  in the blended samples which is attributed to the CH<sub>2</sub> asymmetric wagging.

### 3.3 EIS results

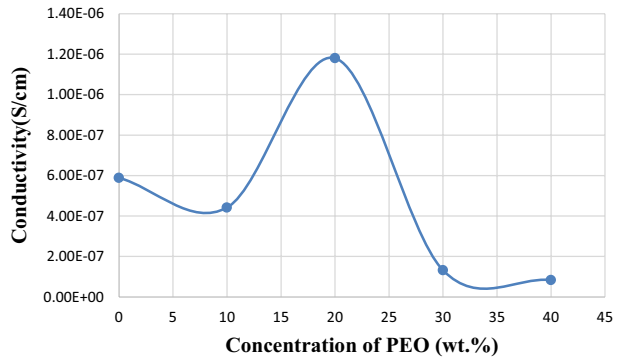
#### 3.3.1 Conductivity results

As mentioned previously, the AC conductivity is a function of polymer concentration, temperature and type of charge carriers and can be calculated using the following equation:

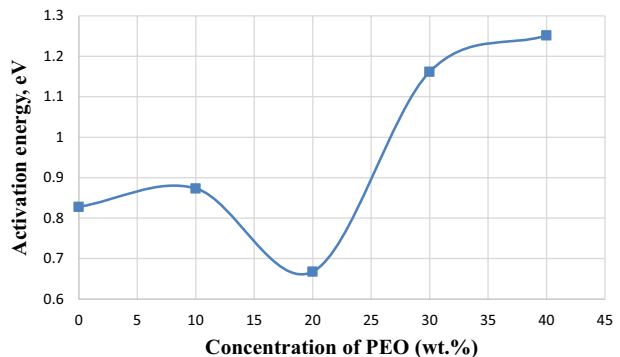
$$\sigma = t/R_b A \quad (2)$$

Where  $t$  is the SPE thickness (cm);  $A$  is the contact area (cm<sup>2</sup>) and  $R_b$  is the bulk resistance (Tang et al. 2010; Pagot et al. 2018). Figure 5-a presents the variation of AC conductivity of plasticized CMC/PEO blends with PEO percentage. The figure showed that by blending of 10 wt% PEO with 90 wt% CMC, the conductivity of pristine CMC increased slightly. However, at higher blending ratios the conductivity is increased to  $1.18\text{E}-06\text{ S/cm}$  and is

**Fig. 5** a and b Dependence of AC conductivity and activation energy on PEO concentration respectively



(a)



(b)

decreased at higher than 20 wt% PEO as presented in Table 4. As large number of protons are provided due to the high degree of dissociation of atoms, and as the amorphousness of prepared films are increased, the conductivity increases. Additionally, decreasing the degree of crystallinity reduces the barrier for the transportation of ions and, hence, the ions transfer rapidly. Accordingly, sample B2 is inferred that it contains a large amorphous fraction.

The dependence of AC conductivity on the blending ratio of polymers gives predictions about the interaction that occurred between CMC, PEO and plasticizer. The observed increase in the conductivity may be attributed to the dissociation of ions which causes the charge carriers' number and mobility to be increased and refers to the strong interaction between the constituent polymers.

### 3.3.2 Temperature dependence of AC conductivity

Dependence of AC conductivity upon temperature has been evaluated to study the mechanism of conduction in the prepared SPEs and to depict the behavior of ions upon heating. The plot of  $\text{Log } \sigma$  against  $1000/T$  for the CMC/PEO SPEs, as shown in Fig. 6, confirms that SPE conductivity is directly proportional to the operating temperature. The reason for increasing conductivity with temperature is attributed to the increase in the free volume through the backbone of the polymer matrix and, hence, the vibrational motion increases. Accordingly, augmentation of mobility and, hence, conductivity happens.

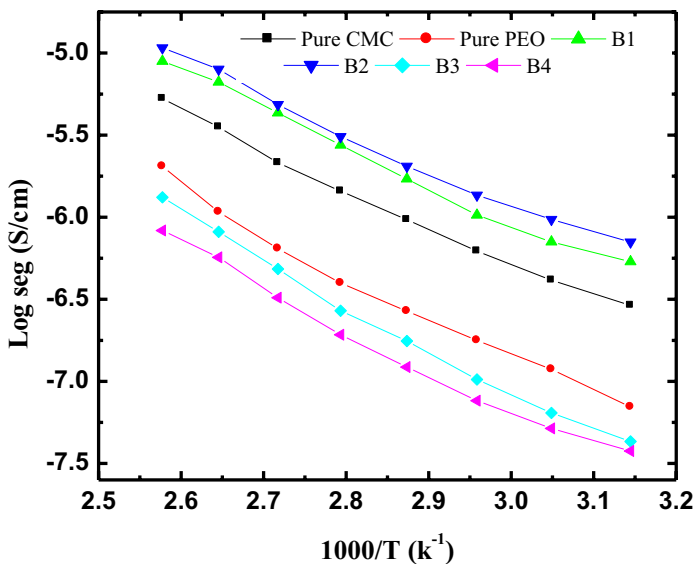


**Fig. 6** Temperature dependence of AC conductivity for pure CMC, pure PEO and CMC/PEO blends as (90:10, 80:20, 70:30 and 60:40)

### 3.3.3 Activation energy

The activation energy  $\Delta E$  is defined as the lowest energy required for charge carrier movement between the valence band and the conduction band which can be calculated using the Arrhenius equation:

$$\sigma_{ac} = \sigma_o e^{-\frac{\Delta E}{kT}} \quad (3)$$

where  $\sigma_o$  is the pre-exponential factor,  $K$  is the Boltzmann constant,  $\Delta E$  is the activation energy and  $T$  is the absolute temperature (Chai and Isa 2015, 2016).

The values of  $\Delta E$  are tabulated in Table 4 and are calculated via the slope of the linear portion of  $\text{Log } \sigma$  with  $1000/T$  plot. The variation of  $\Delta E$  with PEO concentration in the blend matrix is presented in Fig. 5b which indicated that sample B2 possesses the highest AC conductivity and the lowest  $\Delta E$  (approximately 0.67 eV for sample B2) values in comparison with other CMC/PEO blending ratios and these results are confirmed by optical band gaps and FTIR results. The decrease in the activation energy values confirms that the amorphous fractions within the polymer blend matrix are enhanced. As proven earlier (Biswal and Singh 2004), it has been found that the low activation energy values proven that the nature of the prepared solid polymer electrolytes is completely amorphous.

### 3.3.4 Dielectric properties

Studying the dielectric properties is very efficient in studying polymeric materials as it confirms the electrical conductivity results. As CMC and PEO are dielectric materials, which means that they are capable of energy storage, measurement of dielectric constant and dielectric loss is very important for such materials. The dielectric constant measures the amount of energy that is stored in the material, while the dielectric loss measures the energy lost. Measuring the capacitance of the CMC/PEO SPEs facilitates the determination of both dielectric constant and dielectric loss. Both dielectric constant and dielectric loss are calculated using the following equations:

$$\epsilon' = C d / \epsilon_o A \quad (4)$$

$$\epsilon'' = \sigma / \epsilon_o \omega \quad (5)$$

where  $C$  is the capacitance of the SPEs under study,  $d$  is the thickness of the sample,  $\epsilon_o$  is the permittivity of free space,  $A$  is the cross-sectional area of the sample, and  $\omega$  is the angular frequency ( $\omega = 2\pi f$ ) (Eisa et al. 2011; Tang et al. 2010).

Figures 7 and 8 present the variation of dielectric constant and dielectric loss with frequency for the prepared SPEs at ambient temperature. The dielectric constant and dielectric loss values are high, medium, and very low in the low, moderate, and high frequency ranges, respectively. The reason for the large values of both quantities in the low frequency region can be due to the reformation of space charges at the interface between the electrode and electrolyte which prevents the charge transfer. This indicated that at low frequencies both electrode and space charge polarization take place. The figure shows that with increasing the frequency, both dielectric constant and loss are decreased continuously until reaching a constant value at about  $10^6$  MHz. At a frequency between 1 and 10 kHz, both quantities decreased rapidly as the charge carriers in the SPEs do not have enough time to

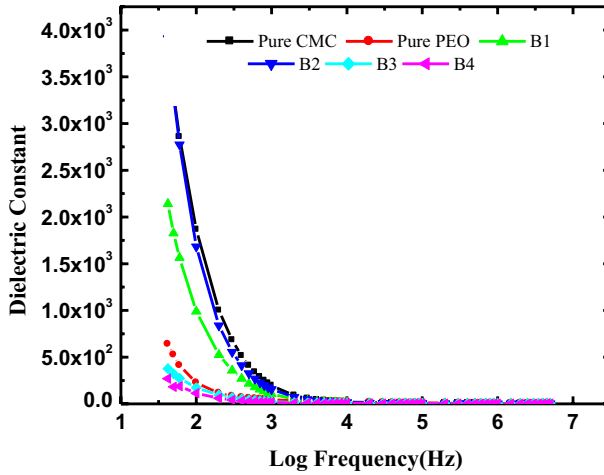


**Fig. 7** Variation of dielectric constant with frequency for pure CMC, pure PEO and CMC/PEO blends as (90:10, 80:20, 70:30 and 60:40)

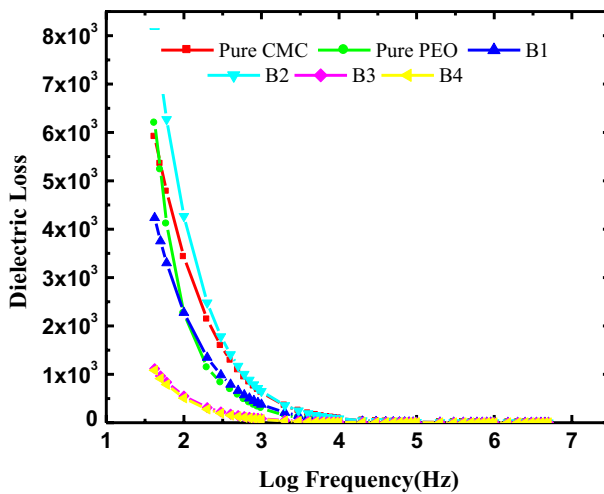


**Fig. 8** Variation of dielectric loss with frequency for pure CMC, pure PEO and CMC/PEO blends as (90:10, 80:20, 70:30 and 60:40)

align themselves in the same direction of the applied field. Therefore, the charges hardly orient themselves due to the rapid reversals of the applied field (Table 5).

Additionally, the figures indicated that the two quantities are functions of blending ratio, where the value of dielectric constant of sample B2 is higher than that of pure PEO but is close to that of pure CMC at low frequencies. However, at lower or higher than 20 wt% PEO, dielectric constant decreased. This increase in the dielectric constant values confirms that the conductivity is enhanced. On the other hand, for dielectric loss and as shown in Fig. 7, sample B2 has a dielectric loss higher than those of pure CMC, pure PEO and other blends. In addition to the low cost of CMC and PEO, the obtained results of UV-Vis,

**Table 5** AC conductivity of plasticized: CMC, PEO and CMC blended with PEO as (90:10, 80:20, 70:30 and 60:40) together with the activation energy at room temperature

Sample	AC conductivity (S/cm)	Activation energy (eV)
Pure CMC	5.89E−07 (Badry et al. 2020)	0.8280 (Badry et al. 2020)
Pure PEO	3.98E−07	0.9957
B1	4.42E−07	0.8734
B2	1.18E−06	0.6677
B3	1.32E−07	1.1615
B4	8.41E−08	1.2513

FTIR and EIS confirm that the blending of CMC and PEO leads to the development of a new type of solid polymer electrolytes that can be used in sensing devices as a membrane material.

## 4 Conclusion

To obtain the optimal composition of the prepared SPEs, different concentrations of CMC and PEO are blended using casting technique. UV–Vis. results indicated that the optical band gap is affected strongly by blending. The formation of chemical bonds between CMC and PEO (hydrogen bonding) is proven by FTIR results. The EIS results revealed that the highest AC conductivity that belongs to sample B2 of (80/20 wt%) measures 1.18E−06 S/cm and that the conductivity increases with increasing temperature due to increasing the mobility of the charge carriers. Dielectric study revealed that both dielectric constant and dielectric loss are decreased with increasing frequency due to the reduction in the number of dipoles with the reversal of the external field. The minimum activation energy obtained was that for the sample containing 80/20 wt% of CMC/PEO which refers to the suitability of this blending ratio to be used as a host polymer matrix in the preparation of SPE. Based on the UV–Vis, FTIR, conductivity and dielectric properties, SPEs of 80 wt% CMC and 20 wt% PEO can be used for the application in the energy storage and sensing devices.

## References

- Armand, M.B.: Polymer electrolytes. *Annu. Rev. Mater. Sci.* **16**, 245–261 (1986)
- Badry, R., Ezzat, H., El-Khodary, S., Morsy, M., Elhaes, H., Nada, N., Ibrahim, M.: Spectroscopic and thermal analyses for the effect of acetic acid on the plasticized sodium carboxymethyl cellulose. *J. Mol. Struct.* **1224**, 129013 (2020)
- Biswal, D.R., Singh, R.P.: Characterisation of carboxymethyl cellulose and polyacrylamide graft copolymer. *Carbohydr. Polym.* **57**, 379–387 (2004)
- Brako, F., Raimi-Abraham, B., Mahalingam, S., Craig, D.Q., Edirisinghe, M.: Making nanofibres of mucoadhesive polymer blends for vaginal therapies. *Eur. Polym. J.* **70**, 186–196 (2015)
- Chahal, R.P., Mahendia, S., Tomar, A.K., Kumar, S.:  $\gamma$ -Irradiated PVA/Ag nanocomposite films: materials for optical applications. *J. Alloys Compd.* **538**, 212–219 (2012)
- Chai, M.N., Isa, M.I.N.: Novel proton conducting solid bio-polymer electrolytes based on carboxymethyl cellulose doped with oleic acid and plasticized with glycerol. *Sci. Rep.* **6**, 27328 (2016)
- Chai, M.N., Isa, M.I.N.: Structural study of plasticized carboxy methylcellulose based solid biopolymer electrolyte. *Adv. Mater. Res.* **1107**, 242–246 (2015)

- Choudhary, S.: Characterization of SiO<sub>2</sub> nanoparticles dispersed (PVA–PEO) blend based nanocomposites as the polymeric nanodielectric materials. *NISCAIR-CSIR*. **23**, 399–410 (2016)
- Choudhary, S.: Structural, optical, dielectric and electrical properties of (PEO–PVP)–ZnO nanocomposites. *J. Phys. Chem. Solids* **121**, 196–209 (2018)
- Dabbak, S.Z., Illias, H.A., Ang, B.C., Abdul Latiff, N.A., Makmud, M.Z.: Electrical properties of polyethylene/polypropylene compounds for high-voltage insulation. *Energies* **11**, 1448 (2018)
- Davis, E.A., Mott, N.: Conduction in non-crystalline systems V. Conductivity, optical absorption and photoconductivity in amorphous semiconductors. *Philos. Mag.* **22**, 0903–0922 (1970)
- Eisa, W.H., Abdel-Moneam, Y.K., Shaaban, Y., Abdel-Fattah, A.A., Zeid, A.M.A.: Gamma-irradiation assisted seeded growth of Ag nanoparticles within PVA matrix. *Mater. Chem. Phys.* **128**, 109–113 (2011)
- El-Bana, M.S., Mohammed, G., El Sayed, A.M., El-Gamal, S.: Preparation and characterization of PbO/carboxymethyl cellulose/polyvinylpyrrolidone nanocomposite films. *Polym. Compos.* **39**, 3712–3725 (2018)
- El-Sayed, S., Mahmoud, K.H., Fatah, A.A., Hassen, A.D.S.C.: DSC, TGA and dielectric properties of carboxymethyl cellulose/polyvinyl alcohol blends. *Physica B: Condens. Matter Phys.* **406**, 4068–4076 (2011)
- Fartode, P.A., Yawale, S.S., Yawale, S.P.: Study of transport and electrical properties of PEO: PVP: NaClO<sub>2</sub> based polymer electrolyte. *Int. J. Chem. Phys. Sci.* **4**, 60–64 (2015)
- Figa, V., Usta, H., Macaluso, R., Salzner, U., Ozdemir, M., Kulyk, B., Krupka, O., Bruno, M.: Electrochemical polymerization of ambipolar carbonyl-functionalized indenofluorene with memristive properties. *Opt. Mater.* **94**, 187–195 (2019)
- Figa, V., Luc, J., Kulyk, B., Baitoul, M., Sahraoui, B.: Characterization and investigation of NLO properties of some selected electrodeposited polythiophenes. *J. Eur. Opt. Soc.* **4**, 09016 (2009)
- Gupta, B., Agarwal, R., Alam, S.M.: Preparation and characterization of polyvinyl alcohol/polyethylene oxide/carboxymethyl cellulose blend membranes. *J. Appl. Polym. Sci.* **127**, 1301–1308 (2013)
- Kargarzadeh, H., Ahmad, I., Abdullah, I., Dufresne, A., Zainudin, S.Y., Sheltami, R.M.: Effects of hydrolysis conditions on the morphology, crystallinity, and thermal stability of cellulose nanocrystals extracted from kenaf bast fibers. *Cellulose J.* **19**, 855–866 (2012)
- Kayyarapu, B., Chekuri, R.: Thermal and conductivity studies of VO<sub>2</sub>+doped methacrylic acid-ethyl acrylate (MAA:EA) copolymer films. *Mater. Res.* **21**, 1 (2018)
- Kulyk, B., Figa, V., Kapustianyk, V., Panasyuk, M., Serkiz, R., Demchenko, P.: Structural properties and temperature behaviour of optical absorption edge in polycrystalline ZnO: X (Cu, Ag) films. *Acta Physica Polonica* **123**, 92–97 (2013)
- Kumar, K.K., Ravi, M., Pavani, Y., Bhavani, S., Sharma, A.K., Rao, V.N.: Investigations on PEO/PVP/NaBr complexed polymer blend electrolytes for electrochemical cell applications. *J. Membr. Sci.* **454**, 200–211 (2014)
- Kumar, K.N., Kang, M., Sivaiah, K., Ravi, M., Ratnakaram, Y.C.: Enhanced electrical properties of polyethylene oxide (PEO) + polyvinylpyrrolidone (PVP): Li + blended polymer electrolyte films with addition of Ag nanofiller. *Solid state ion.* **22**, 815–825 (2016)
- Kumar, R.: Enhancement in electrical properties of PEO based nano-composite gel electrolytes. *J. Mater. Sci.* **2**, 12 (2014)
- Li, W., Pang, Y., Liu, J., Liu, G., Wang, Y., Xia, Y.: A PEO-based gel polymer electrolyte for lithium ion batteries. *Rsc Adv.* **7**, 23494–23501 (2017)
- Ling, Y., Tian, Y., Wang, X., Wang, J.C., Knox, J.M., Perez-Orive, F., Du, Y., Tan, L., Hanson, K., Ma, B., Gao, H.: Enhanced optical and electrical properties of polymer-assisted all-inorganic perovskites for light-emitting diodes. *Adv. Mater.* **28**, 8983–8989 (2016)
- Masoud, E.M., El-Bellihi, A.A., Bayoumy, W.A., Mousa, M.A.: Effect of LiAlO<sub>2</sub> nanoparticle filler concentration on the electrical properties of PEO–LiClO<sub>4</sub> composite. *Mater. Res. Bulletin.* **48**, 1148–1154 (2013)
- Meyer, W.H.: Polymer electrolytes for lithium/ion batteries. *Adv. Mater.* **10**, 439–448 (1998)
- Mishra, R.K., Mishra, P., Verma, K., Joseph, K.: Manipulation of thermo-mechanical, morphological and electrical properties of PP/PET polymer blend using MWCNT as nano compatibilizer: a comprehensive study of hybrid nanocomposites. *Vacuum* **157**, 433–441 (2018a)
- Mishra, R.K., Mishra, P., Verma, K., Joseph, K.: Manipulation of thermo-mechanical, morphological and electrical properties of PP/PET polymer blend using MWCNT as nano compatibilizer: a comprehensive study of hybrid nanocomposites. *Vacuum J.* **157**, 433–441 (2018b)
- Mohan, V.M., Bhargav, P.B., Raja, V., Sharma, A.K., Narasimha Rao, V.V.R.: Optical and electrical properties of pure and doped PEO polymer electrolyte films. *Soft Mater.* **5**, 33–46 (2007)

- Morsi, M.A., Abdelaziz, M., Oraby, A.H., Mokhles, I.: Structural, optical, thermal, and dielectric properties of polyethylene oxide/carboxymethyl cellulose blend filled with barium titanate. *J. Phys. Chem. Solids* **125**, 103–114 (2019)
- Morsi, M.A., El-Khodary, S.A., Rajeh, A.: Enhancement of the optical, thermal and electrical properties of PEO/PAM: Li polymer electrolyte films doped with Ag nanoparticles. *Physica B: Condens. Matter Phys.* **539**, 88–96 (2018)
- Mott, N.F.: Conduction in non-crystalline systems: IV. Anderson localization in a disordered lattice. *Philos. Mag.* **22**, 7–29 (1970)
- Murri, R., Schiavulli, L., Pinto, N., Ligonzo, T.: Urbach tail in amorphous gallium arsenide films. *J. Non-Cryst. Solids* **139**, 60–66 (1992)
- Nasution, T.I., Asrosa, R., Machrina, Y., Nainggolan, I., Balyan, M., Rumansyah, R.: Improved electrical properties of chitosan based acetone sensor by adding carboxymethylcellulose (CMC). *MS&E*. **180**, 012018 (2017)
- Ngai, K.S., Ramesh, S., Ramesh, K., Juan, J.C.: A review of polymer electrolytes: fundamental, approaches and applications. *Ionics* **22**, 1259–1279 (2016)
- Pagot, G., Bertasi, F., Vezzù, K., Nawn, G., Pace, G., Nale, A., Di Noto, V.: Correlation between properties and conductivity mechanism in poly (vinyl alcohol)-based lithium solid electrolytes. *Solid State Ion* **320**, 177–185 (2018)
- Samsudin, A.S., Isa, M.I.: Structural and electrical properties of carboxy methylcellulose-dodecyltrimethyl ammonium bromide-based biopolymer electrolytes system. *Int. J. Polym. Mater.* **61**, 30–40 (2012)
- Selvasekarapandian, S., Baskaran, R., Kamishima, O., Kawamura, J., Hattori, T.: Laser Raman and FTIR studies on Li<sup>+</sup> interaction in PVAc–LiClO<sub>4</sub> polymer electrolytes. *Spectrochim. Acta A*. **65**, 1234–1240 (2006)
- Sengwa, R.J., Choudhary, S.: Dielectric and electrical properties of PEO–Al<sub>2</sub>O<sub>3</sub> nanocomposites. *J. Alloy. Compd.* **701**, 652–659 (2017)
- Sharma, P., Kanchan, D.K., Gondaliya, N.: Effect of ethylene carbonate concentration on structural and electrical properties of PEO–PMMA polymer blends. *Ionics* **19**, 777–785 (2013)
- Srivastava, N., Tiwari, T.: New trends in polymer electrolytes: a review. *Polymers* **9**, 1 (2009)
- Tang, N., Kuo, W., Jeng, C., Wang, L., Lin, K., Du, Y.: Coil-in-coil carbon nanocoils: 11 gram-scale synthesis, single nanocoil electrical properties, and electrical contact improvement. *ACS Nano* **4**, 781–788 (2010)
- Zhu, C., Chen, J., Koziol, K.K., Gilman, J.W., Trulove, P.C., Rahatekar, S.S.: Effect of fibre spinning conditions on the electrical properties of cellulose and carbon nanotube composite fibres spun using ionic liquid as a benign solvent. *Express Polymer Lett.* **8**, 1 (2014)

**Publisher's Note** Springer Nature remains neutral with regard to jurisdictional claims in published maps and institutional affiliations.